Engineering and Applied Sciences
2023; 8(3): 36-46
http://www.sciencepublishinggroup.com/j/eas
doi: 10.11648/j.eas.20230803.11
ISSN: 2575-2022 (Print); ISSN: 2575-1468 (Online)

Behavior of Fiber Reinforced Polymer (FRP) Confined Crumb Rubber Concrete at Elevated Temperatures

Mohammed Faruqi, Ajibola Habeeb Alamutu, Breanna Bailey, Francisco Aguiniga

Department of Civil and Architectural Engineering, Texas A & M University-Kingsville, Kingsville, USA

Email address:
m-faruqi@tamuk.edu (Mohammed Faruqi)

To cite this article:
Mohammed Faruqi, Ajibola Habeeb Alamutu, Breanna Bailey, Francisco Aguiniga. Behavior of Fiber Reinforced Polymer (FRP) Confined Crumb Rubber Concrete at Elevated Temperatures. *Engineering and Applied Sciences*. Vol. 8, No. 3, 2023, pp. 36-46.
doi: 10.11648/j.eas.20230803.11

Received: May 11, 2023; **Accepted**: May 30, 2023; **Published**: June 9, 2023

Abstract: Researchers in engineering and sciences have consistently carried out relevant studies on different ways to minimize the use of natural resources and to control environmental pollution. Aggregates used in concrete are generally obtained from rocks while huge collection of scrap tires are one of the biggest form of wastes in our societies throughout the world. Studies have shown that aggregates in conventional concrete (CC) can be partially replaced with crumb rubber particles. This type of concrete can be referred to as Crumb Rubber Concrete (CRC). Confinement of crumb rubber concrete and conventional concrete have shown to increase their compressive strengths. However, the behavior of CRC confined with Carbon Fiber Reinforced Polymer (CFRP) sheets at elevated temperatures is still unknown. The knowledge and application of this could lead to a cost-effective and practical consideration in fire safety design. Therefore, this study examines the confined compressive strength of CRC confined with CFRP sheets at elevated temperatures. Finite Element Models (FEM) of CC and CRC with and without confinement were developed at room temperature and validated with literature, American Concrete Institute (ACI), and an indirect reference to the real behavior of the material. FEM results agreed reasonably with these sources. Finite element models of confined CC and confined CRC were subjected to elevated temperature and compared with the finite element model of confined CC and confined CRC respectively at room temperature. It was found that models under service confined compressive stress subjected to elevated temperature of 120°C experienced strength loss in the range of 46% to 51% when compared with the room temperature. Accordingly, a strength loss in the range of 34% to 56% was observed for models under maximum confined compressive stress. An example of an axially loaded CFRP-confined CRC column with explanations to calculate the nominal load capacity of a modeled column at room temperature and elevated temperature using our data was also carried out. The percentage difference between the calculated and the model were respectively 3% and 12.1% at room and elevated temperature.

Keywords: Carbon Fiber Reinforced Polymer, Conventional Concrete, Crumb Rubber Concrete, Elevated Temperatures, Compressive Strength

1. Introduction

The stockpile production of scrap tires in the United States has sufficiently reduced over time as a result of its demand in the production of Tire Derived Fuels (TDF), civil engineering construction, and other areas [1]. In addition to the known application of scrap tires to civil engineering, crumb rubber derived from treating and processing scrap tires is used to partially replace aggregates in concrete. Researchers [2-4] have shown that Crumb Rubber Concrete (CRC) with less than 25% of aggregates replaced by rubber have acceptable compressive strength without any additive to optimize strength of the concrete mix. An increase in the rubber content of CRC results in decrease of compressive strength, increase in ductility, energy dissipation ability, damping ratio, and impact resistance [3, 5]. Additional studies [6-8] on CRC have also reported improvements, when compared with conventional concrete. These attributes make CRC with high rubber content suitable for the construction of concrete members subjected to dynamic loading such as columns in earthquake zones and highway barriers [2, 5]. Studies [2-4] have shown that confining CRC with Fiber Reinforced Polymer (FRP) sheets increases its compress compressive strength while the suitable properties of CRC are retained.

Crumb rubber concrete loses 96 kg/m^3 in unit weight for every 23 kg of crumb rubber added to concrete mix [9], thus a reduction in the compressive strength. Another research [10] stated that the compressive strength of CRC with full replacement of fine aggregates with crumb rubber and optimized with a binder material is 160% of the compressive strength of the non-optimized CRC also with full replacement of fine aggregates. Panels made with CRC is said to have higher sound absorption and lower heat transfer properties compared to the panels made from conventional concrete [11]. This is because conventional aggregates are pretreated and washed in order to remove unwanted elements that can be detrimental to the mechanical properties of conventional concrete. Studies [12, 13] have also shown that surface modification of crumb rubber and the addition of silica fume to CRC mix helps improve the mechanical properties of CRC.

Fiber reinforced plastics (FRPs) are generally suitable as confining jackets to structural members because of their continuous increase in confining action due to elastic behavior up to failure and resistance to corrosion [3, 4]. These plastics can be simply defined as composite materials containing one or more fiber types embedded in a polymer matrix [14]. The fibers have high strength. The properties of FRPs which make them suitable in structural engineering are: resistant to corrosion, high strength to weight ratio, good fatigue features, high tensile strength, and ease of construction. In structural applications, FRP bars have considerably been studied [15-18] at room and elevated temperatures. They are used internally in the construction of structural members as bars or in retrofitting existing structural members as sheets, which is the focus of this study. Sheets of FRPs can be classified according to the orientation of the fibers as unidirectional or woven (bidirectional). When FRP sheets are applied to member in the transverse direction; the shear capacity, ductility, and compressive strength of such member is improved but when FRP sheets are applied in the longitudinal direction of the structural member, the flexural capacity of the member is improved [14]. Study [2] shows that confining conventional concrete with one, two, and three layers of Unidirectional (UD) Carbon FRP (CFRP) in the transverse direction increases the compressive strength by 45%, 111%, and 156% respectively and confining CRC with one, two, and three layers of CFRP in the transverse direction increases the compressive strength by 59%, 116%, and 160% respectively. Another study [19] also shows that confining conventional concrete with one, two, three, and four layers of CFRP increases the compressive strength by 100%, 141%, 221%, and 267% respectively. This, in summary, tells us that an increase in CFRP thickness increases the compressive strength of concrete.

Studies [2-5, 9-14] have established that the thermo mechanical properties of FRP sheets are dependent on the polymer matrix type used in manufacturing the FRP sheets. Polymer matrix (resin) becomes softs when FRP sheets are subjected to temperature close the glass transition temperature T_g of the resin, which limits the transfer of stress between fibers and causes debond between FRP sheet and concrete. Glass transition temperature is the temperature at which the FRP polymer resin undergoes a change from being hard and brittle to being viscous and rubbery [14].

In the past, fire safety specifications for structural members were met by making sure the structural members satisfy specific fire ratings, which are obtained by conducting full-scale fire-tests that are non-economical. In recent times, performance-based design methods are employed. These involve conducting detailed calculations and simulations instead of the full-scale fire tests as economic necessity. Analytical models derived must then be proven using results from past full-scale tests prior to application [20].

Researchers [2-5, 9-14, 19, 20] have carried out experimental analyses with the development of analytical models to support their experiments but little study has been carried out on finite element modeling of test cases and their behavior at elevated temperatures. Therefore, this work makes an attempt to look into this.

2. Finite Element Modeling (FEM) and Description of Model

A simple approach of FEM using ANSYS was taken which can also be easily adapted for future researches to broaden the knowledge and scope of the subject matter. The following basic guidelines were used for modeling the axially loaded specimens in compression: a) define constants; b) material properties; c) create the FE mesh which establishes element numbers and nodes; d) define boundary condition/constraint, load type and load steps, and e) identify the unknown quantities.

A total of eight solid concrete cylinders, 100mm in diameter and 200mm in depth, were modeled and analyzed using SpaceClaim and Mechanical APDL respectively in Static Structural Project Workflow under ANSYS Workbench 18.1. Carbon FRP were modeled as hollow cylinders (shell) of thickness 0.13mm per layer and 200mm depth that are concentric and perfectly bonded to the concrete cylinders. Four cylinders were control cylinders. The control cylinders consisted of conventional concrete with no crumb rubber aggregates and the other four cylinders consisted of crumb rubber as partial aggregates.

The dimensions used for modeling were based on literature [2] and ASTM C39-05 [21]. For the control concrete cylinders, one had no CFRP layer, one had one layer of CFRP, one had two layers of CFRP, and the last one had three layers of CFRP. Also for the CRC, one had no CFRP layer, one had one layer of CFRP, one had two layers of CFRP, and the last one had three layers of CFRP. To validate the FE models developed using the properties in literature [2], the models were loaded to failure, f_c' (28 days maximum unconfined com-pressive strength) and f_{cc}' (28 days maximum confined compre-ssive strength). These values were recorded and compared to the values in literature and ACI. Upon validation, the models were then re-analyzed with increasing temperature and with the confined service stresses (f_{cc}) in the

conventional concrete and CRC less than $0.65f'_{cc}$ as specified by section 12.1.3 of ACI 440.2R-08 [22]. This is to avoid damage to the specimens in form of notable cracking in the radial direction.

2.1. Modeling Using SpaceClaim

The concrete cylinders modeled here are solid cylinders created by defining circular surface of 100mm diameter in the xz-plane and extruding the surface 200mm in depth along y-axis. CFRP are modeled as cylindrical shells with inner radius 0.13mm less than the outer radius for the first, second, and third layers. Circular surfaces with diameters 100.13mm, 100.26mm, and 100.39mm were created for first layer, second layer, and third layer respectively in the xz-plane. The circular surfaces were then extruded 200mm in depth along the y-axis to form initial solid cylinders. Carbon FRP cylindrical shells were moved to coincide with the concrete cylinder and become concentric shapes to be specified as perfectly bonded during analysis. Figure 1 shows the plan and isometric views of a concrete cylinder with one layer CFRP cylindrical shell.

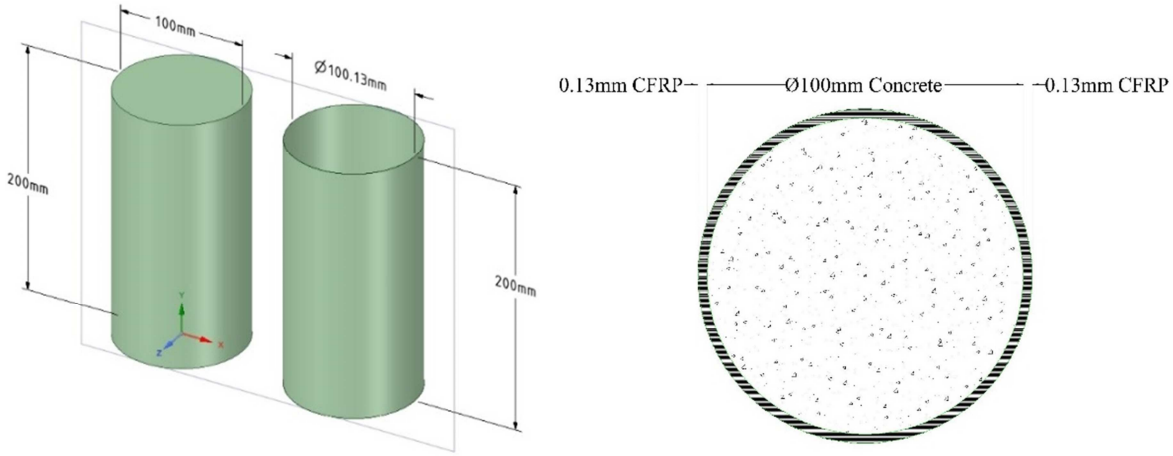

Figure 1. *Concrete-CFRP Geometry Modeled in SpaceClaim. (a) Isometric; and (b) Plan View.*

2.2. Analysis Using Mechanical APDL in ANSYS Workbench

The geometry of the concrete cylinders were automatica-lly imported into the Mechanical APDL upon opening the model tab of the project workflow. The properties of the materials used in this analysis were obtained from literature [2]. Materials properties are shown in Table 1.

Table 1. *Material Properties [2].*

Material Properties					
Material	$E_c(MPa)$	$f'_c(MPa)$	$f_r(MPa)$	ε_c	ν
CC	42,508	53.5	4.6	0.00243	0.20
CRC	36,434	41.6	4.8	0.00206	0.21
Material	$E_f(MPa)$	$f'_c(MPa)$	$f_{fu}(MPa)$	ε_{fu}	ν
CFRP	230,000	-	4900	0.02100	0.30

E_c, f_r, ε_c, E_f, f_{fu}, ε_{fu} and ν from Table 1 are Young's modulus of concrete, modulus of rupture of concrete, strain in unconfined concrete, Young's modulus of FRP, maximum tensile strength of FRP, ultimate strain in FRP, and materials Poisson's ratio respectively. Equations [23] were used to obtain compressive uniaxial stress-strain data for the concrete specimens in this study. The defined material properties were assigned to their respective geometry accordingly. Surface to surface connection was automatically detected and defined between the concentric (concrete and CFRP) geometry imported from SpaceClaim. For the connection, concrete was defined as the target body tied to CFRP. Figure 2 shows the concrete and CFRP surfaces. In order to simulate nonlinearity of contact, nonlinear mechanical method of meshing was used in analysis. Nonlinear mechanical meshing tends to provide fewer lower quality elements. The meshing process divided confined models into 4800 elements with 19558 nodes for one layer CFRP models, 5460 elements with 20944 nodes for two layers CFRP models, 6100 elements with 22288 nodes, and each unconfined model into 9150 elements with 38,981 nodes. Smaller mesh size was used for the unconfined concrete models. This is because the solution would be more accurate and faster to compute. Figure 3 shows typical mesh generated for the concrete models. Fixed support was applied to the bottom surface of the models as boundary conditions to resist the bottom against any form of displacement and rotation when loaded. Load was applied in incremental steps to help in the convergence of solution.

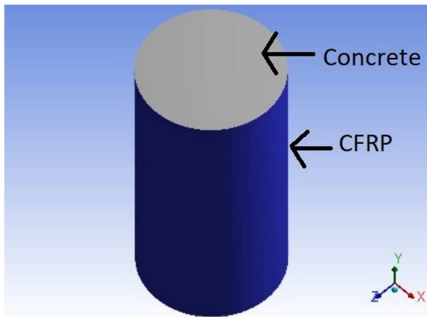

Figure 2. *Concrete and CFRP Surfaces.*

Figure 4 shows pressure and boundary condition at their

applied surfaces. After the boundary conditions and loading were defined, the models were solved for compressive stress and strain. Figures 5, 6, 7, and 8 show the stresses develop-ed in the models.

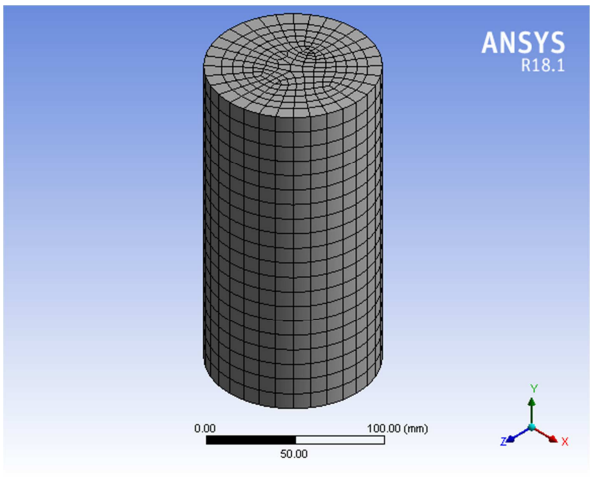

Figure 3. *Meshing of the Concrete Cylinder Model in Isometric View.*

The compressive stress in each model is calculated as the approximate average of the stress range in which majority of elements in a model fall. Stress singularities at the top and bottom of the models are results of the bottom restraint (fixed support), loading applied at the top of the model, and the contact between CFRP and concrete geometry (edges of the bottom elements). Such stresses increase with refinement of mesh size and according to St. Venant's Principle, which states that the effect of local disturbance to a uniform stress field remains local [24]. Figure 9 illustrates the principle. This implies that the true results of the models will not be disturbed at locations away from the local stress at the top and bottom of the models. This permits us to calculate the compressive stresses.

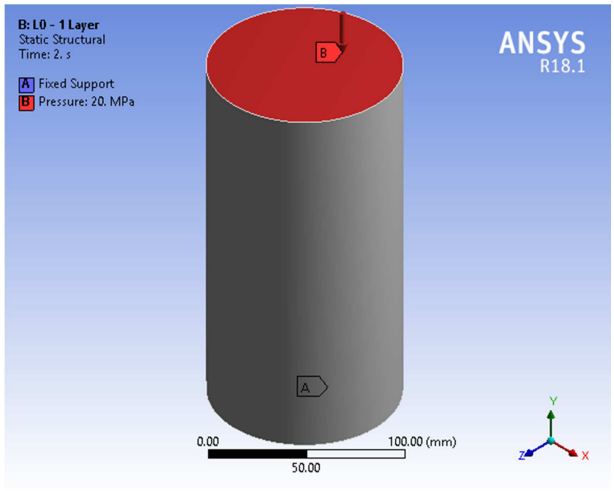

Figure 4. *Static Structural Loading and Boundary Condition.*

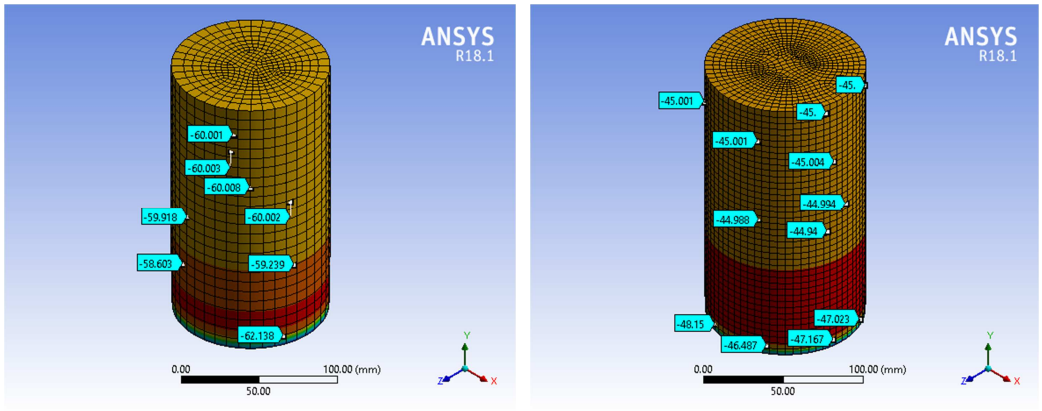

Figure 5. *Unconfined Compression Models. (a) CC; and (b) CRC.*

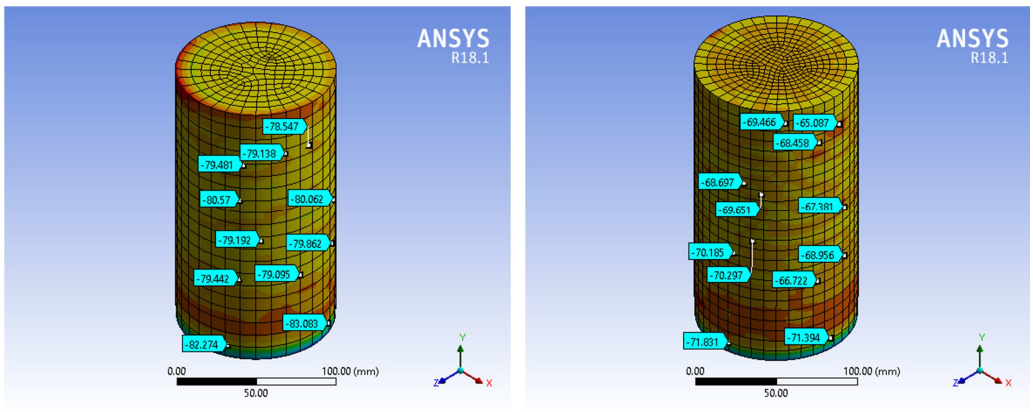

Figure 6. *Confined compression models. (a) CC 1 Layer CFRP; and (b) CRC 1 Layer CFRP.*

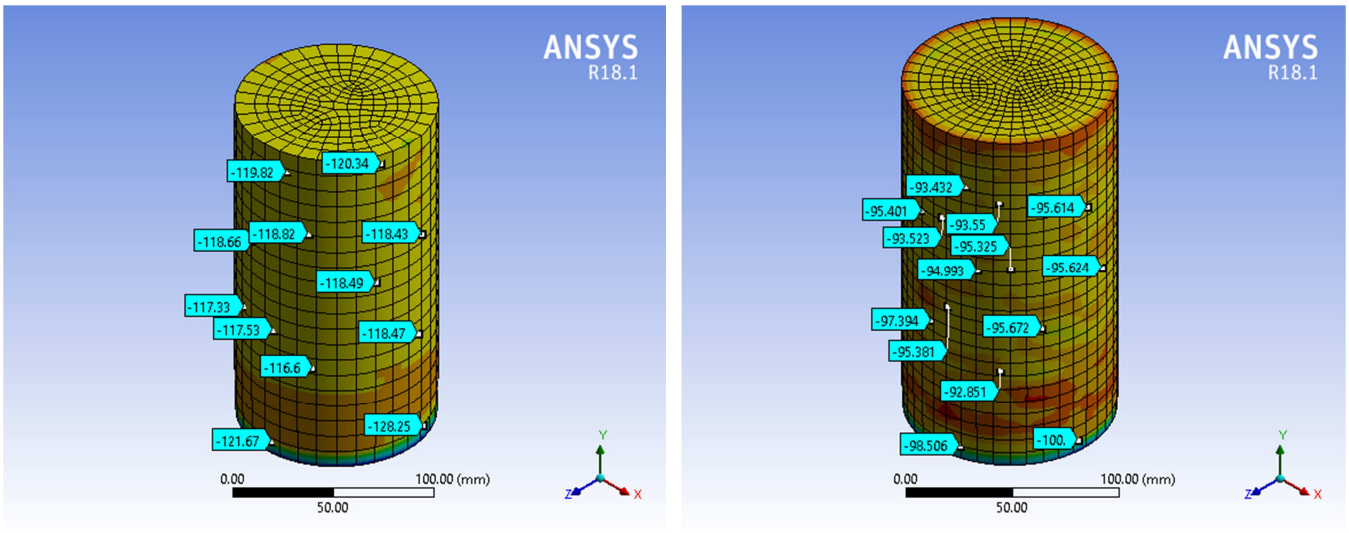

Figure 7. *Confined Compression Models. (a) CC 2 Layers CFRP; and (b) CRC 2 Layers CFRP.*

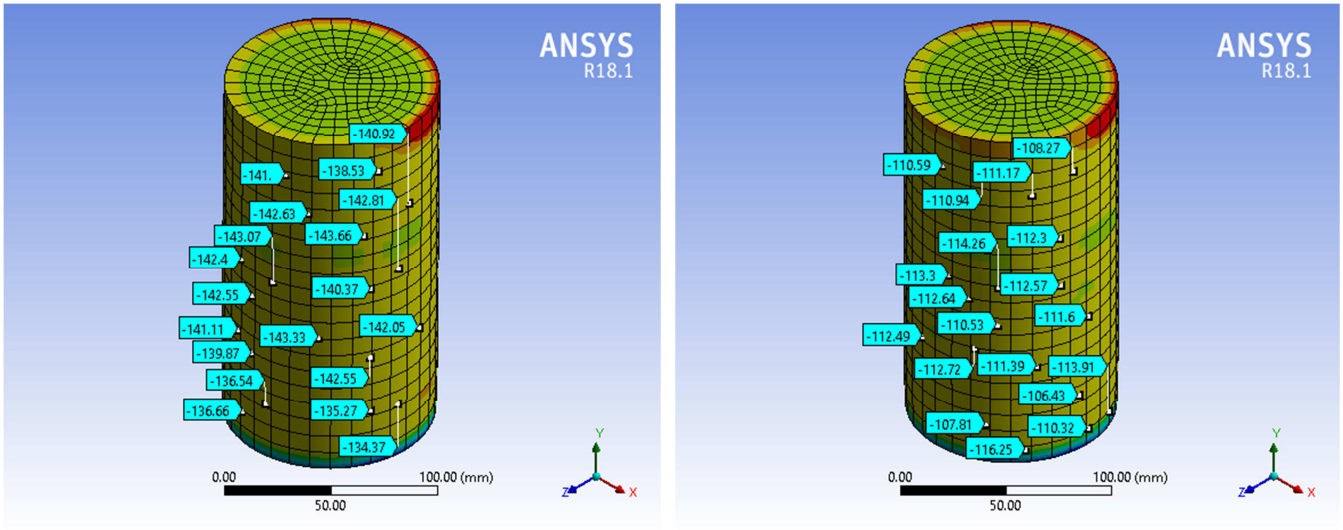

Figure 8. *Confined Compression Models. (a) CC 3 Layers CFRP; and (b) CRC 3 Layers CFRP.*

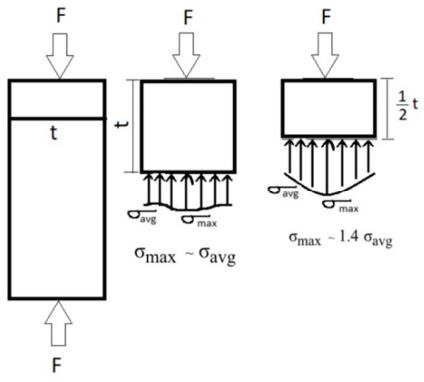

Figure 9. *Illustration of St. Venant's Principle.*

3. Comparison of Models

3.1. Comparison with Literature

Table 2 provides a summary of the maximum compressive stress developed in each model in comparison with literature [2]. It can be seen from Table 2 that the compressive strength values obtained from finite element modeling agrees closely with the literature. The compressive strengths of unconfined conventional concrete and crumb rubber concrete for the FE models are 12.5% and 12.1% greater than literature values respectively and the compressive strengths of the confined conventional concrete and crumb rubber concrete for the FE models are 2% to 5.7% greater than literature values.

Table 2. *Comparison of FEM with Literature.*

Model Name	Compressive stresses in MPa		
	FEM f_c'	Literature [2] f_c'	$\frac{f_c'(FEM)}{f_c'(Literature)}$
Unconfined CC	60.20	53.50	1.125
Unconfined CRC	46.65	41.60	1.121

Model Name	FEM f'_{cc}	Literature [2] f'_{cc}	$\frac{f'_{cc}(FEM)}{f'_{cc}(Literature)}$
CC 1 layer	79.96	77.60	1.030
CRC 1 layer	68.19	66.20	1.030
CC 2 layers	119.40	113.00	1.057
CRC 2 layers	95.17	90.00	1.057
CC 3 layers	139.91	137.00	1.021
CRC 3 layers	110.13	108.00	1.020

3.2. Comparison with ACI Code

The loadings and compressive stress values obtained from finite element modeling are compared with the values obtained using analytical models in chapter 12 of ACI 440.2R-08 [22]. This is to validate the FEM values before applying elevated temperatures to the models in ANSYS. These equations are shown as 1, 2, and 3:

$$f'_{cc} = f'_c + \psi_f 3.3 \kappa_a f_l \quad (1)$$

where ψ_f is the additional reduction factor for confining pressure, κ_a is the efficiency factor for the geometry of section, and f_l is the FRP confining pressure. $\psi_f = 0.95, \kappa_a = 1$ for circular cross sections. The FRP confining pressure used in this equation is calculated as:

$$f_l = \frac{2E_f n t_f \varepsilon_{fe}}{D} \quad (2)$$

$$\varepsilon_{fe} = \kappa_\varepsilon \varepsilon_{fu} \quad (3)$$

where n is the number of FRP layer, t_f is the thickness of FRP sheet for one layer, ε_{fe} is the effective FRP strain, κ_ε is efficiency factor of FRP strain which accounts for the premature failure of FRP sheet, D is the diameter of concrete models. $\kappa_\varepsilon = 0.586$ for CFRP. For FRP confinement action to be valid, the ratio $\frac{f_l}{f'_c} > 0.08$, and the ultimate confined concrete strain, $\varepsilon_{ccu} \leq 0.01$.

Calculating maximum confined compressive stress for conventional concrete and crumb rubber concrete:

For CC 1 layer,

$$n = 1, f_{fu} = 4900\ MPa, \varepsilon_{fu} = 0.021$$

$$t_f = 0.13mm, E_f = 230\ GPa, D = 100mm.$$

$$f'_c = 53.5\ MPa$$

$$\varepsilon_{fe} = 0.586 \times 0.021 = 0.012306$$

$$f_l = \frac{2 \times 230 \times 10^3 \times 1 \times 0.13 \times 0.012306}{100} = 7.36\ MPa$$

$$\frac{f_l}{f'_c} = \frac{7.36}{53.5} = 0.14 > 0.08;$$

therefore

$$f'_{cc} = 53.5 + 0.95 \times 3.3 \times 1 \times 7.36 = 76.57\ MPa$$

For CC 2 layers,

$$n = 2, f_{fu} = 4900\ MPa, \varepsilon_{fu} = 0.021$$

$$t_f = 0.13mm, E_f = 230\ GPa, D = 100mm.$$

$$f'_c = 53.5\ MPa$$

$$\varepsilon_{fe} = 0.586 \times 0.021 = 0.012306$$

$$f_l = \frac{2 \times 230 \times 10^3 \times 2 \times 0.13 \times 0.012306}{100} = 14.72\ MPa$$

$$\frac{f_l}{f'_c} = \frac{14.72}{53.5} = 0.28 > 0.08;$$

therefore

$$f'_{cc} = 53.5 + 0.95 \times 3.3 \times 1 \times 14.72 = 99.65\ MPa$$

For CC 3 layers,

$$n = 3, f_{fu} = 4900\ MPa, \varepsilon_{fu} = 0.021$$

$$t_f = 0.13mm, E_f = 230\ GPa, D = 100mm.$$

$$f'_c = 53.5\ MPa$$

$$\varepsilon_{fe} = 0.586 \times 0.021 = 0.012306$$

$$f_l = \frac{2 \times 230 \times 10^3 \times 3 \times 0.13 \times 0.012306}{100} = 22.08\ MPa$$

$$\frac{f_l}{f'_c} = \frac{22.08}{53.5} = 0.41 > 0.08;$$

therefore

$$f'_{cc} = 53.5 + 0.95 \times 3.3 \times 1 \times 22.08 = 122.72\ MPa$$

For CRC 1 layer,

$$n = 1, f_{fu} = 4900\ MPa, \varepsilon_{fu} = 0.021$$

$$t_f = 0.13mm, E_f = 230\ GPa, D = 100mm.$$

$$f'_c = 41.6\ MPa$$

$$\varepsilon_{fe} = 0.586 \times 0.021 = 0.012306$$

$$f_l = \frac{2 \times 230 \times 10^3 \times 1 \times 0.13 \times 0.012306}{100} = 7.36\ MPa$$

$$\frac{f_l}{f'_c} = \frac{7.36}{53.5} = 0.14 > 0.08;$$

therefore

$$f'_{cc} = 41.6 + 0.95 \times 3.3 \times 1 \times 7.36 = 64.67\ MPa$$

For CRC 2 layers,

$$n = 2, f_{fu} = 4900\ MPa, \varepsilon_{fu} = 0.021$$

$$t_f = 0.13mm, E_f = 230\ GPa, D = 100mm.$$

$$f_c' = 41.6\ MPa$$

$$\varepsilon_{fe} = 0.586 \times 0.021 = 0.012306$$

$$f_l = \frac{2\times230\times10^3\times2\times0.13\times0.012306}{100} = 14.72\ MPa$$

$$\frac{f_l}{f_c'} = \frac{14.72}{53.5} = 0.28 > 0.08;$$

therefore

$$f_{cc}' = 41.6 + 0.95 \times 3.3 \times 1 \times 14.72 = 87.75\ MPa$$

For CRC 3 layers,

$$n = 3, f_{fu} = 4900\ MPa, \varepsilon_{fu} = 0.021$$

$$t_f = 0.13mm, E_f = 230\ GPa, D = 100mm.$$

$$f_c' = 41.6\ MPa$$

$$\varepsilon_{fe} = 0.586 \times 0.021 = 0.012306$$

$$f_l = \frac{2\times230\times10^3\times3\times0.13\times0.012306}{100} = 22.08\ MPa$$

$$\frac{f_l}{f_c'} = \frac{22.08}{53.5} = 0.41 > 0.08;$$

therefore

$$f_{cc}' = 41.6 + 0.95 \times 3.3 \times 1 \times 22.08 = 110.82\ MPa$$

Comparison between FEM and ACI results is shown in Table 3.

Table 3. *Comparison Between FEM & ACI.*

Conventional Concrete Stresses (MPa)			
Name	$f_{cc}'(FEM)$	$f_{cc}'(ACI)$	$\frac{f_{cc}'(FEM)}{f_{cc}'(ACI)}$
CC 1 layer	79.96	76.57	1.044
CC 2 layers	119.40	99.65	1.198
CC 3 layers	139.91	122.72	1.140

Crumb Rubber Concrete Stresses (MPa)			
Name	$f_{cc}'(FEM)$	$f_{cc}'(ACI)$	$\frac{f_{cc}'(FEM)}{f_{cc}'(ACI)}$
CRC 1 layer	68.19	64.67	1.054
CRC 2 layers	95.17	87.75	1.085
CRC 3 layers	110.13	110.82	0.994

The average percentage difference between the FEM and ACI results for the conventional and crumb rubber concrete are 12.73% and 4.43% respectively.

3.3. Comparison with an Indirect Reference

Analytical model suggested in study [25] was used as an indirect reference to also validate our FE model results. This indirect reference is valid for cylindrical concrete specimens with unconfined compressive strength ranging from 18MPa to 64MPa and confined compressive strength ranging from 33MPa to 240MPa for carbon, aramid, and glass fiber reinforced polymer sheets. The average percentage difference between FEM results and the results of the suggested model in the study for conventional concrete and crumb rubber concrete are 3.73% and 8.2% respectively, which is a reasonable agreement to the finite element models.

4. Finite Element Modeling at Elevated Temperatures and Results

General purpose carbon fiber-epoxy resin composite sheets are thermosets that usually have glass transition temperature less than 200°C while carbon fibers as a constituent have higher glass transition temperature. This is because the epoxy polymer matrix degrades in mechanical properties at glass transition temperatures lower than that of carbon fiber thereby causing inability to transfer stress from one fiber to another in the composite. The temperature range used in this study is 100°C to 140°C as the decrease in mechanical properties of carbon fiber-epoxy composite sheets becomes pronounced at temperatures slightly above 100°C according to literature [14]. The room temperature, which is also referred to as environment temperature, at which the compressive strengths of concrete specimens were obtained is 22°C. At this room temperature, it is assumed that no thermal strains occurred in materials studied.

To simulate a practical stress condition scenario for the elevated temperature modeling, the models were loaded such that the service stresses in the confined concrete specimens are approximately $0.60f_{cc}'$ as specified by ACI code in our earlier discussion. The coefficient of thermal expansion of concrete specimen and CFRP used in this study are $1.4 \times 10^{-5}\mathrm{C}^{-1}$ and $3.0 \times 10^{-5}\mathrm{C}^{-1}$ respectively. A steady state thermal condition of 120°C was applied to the whole specimen. The thermal condition represents the average of the temperature range mentioned above. Figures 10, 11, and 12 illustrate the simulations of loaded models at a temperature of 120°C.

The confined compressive stress of each model is calculated as the average of the stresses in all elements except the bottom and top elements. The top and bottom element are excluded from this calculation because of local stresses

developed as a result of loading at the top and the fixed support at the bottom.

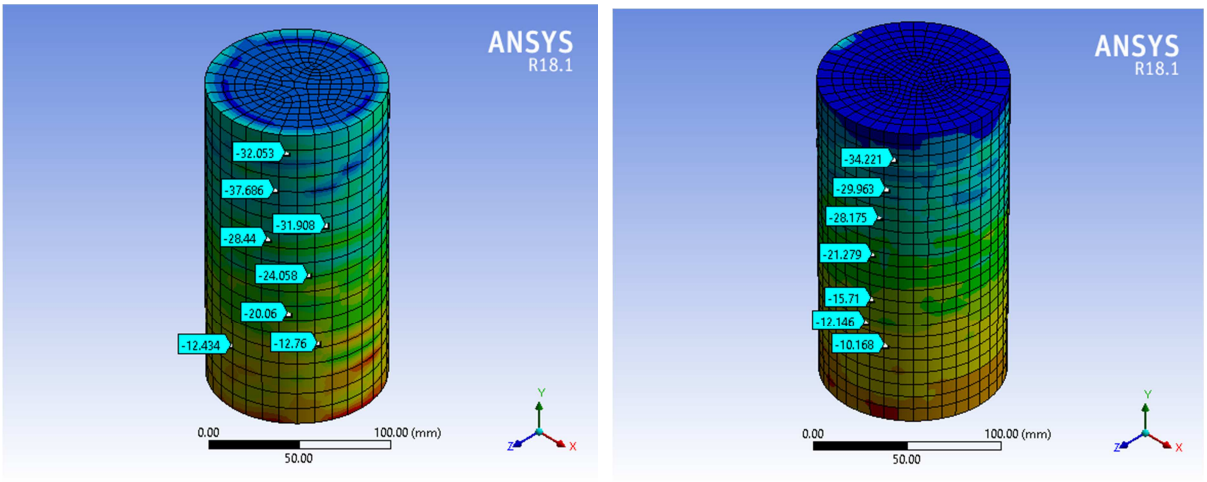

Figure 10. *Heated Compression Models. (a) CC 1 Layer; and (b) CRC 1 Layer.*

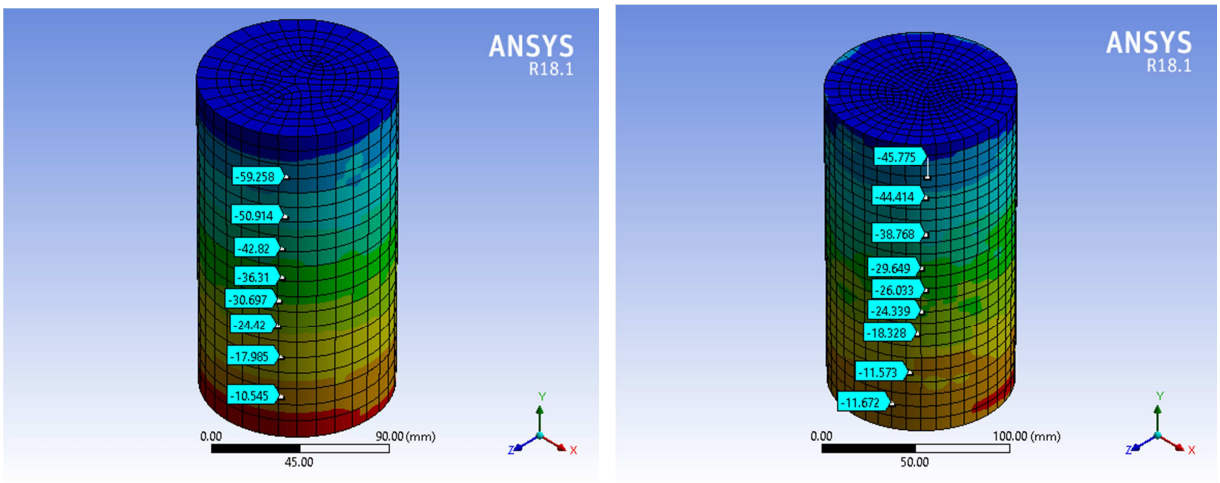

Figure 11. *Heated Compression Models. (a) CC 2 Layers; and (b) CRC 2 Layers.*

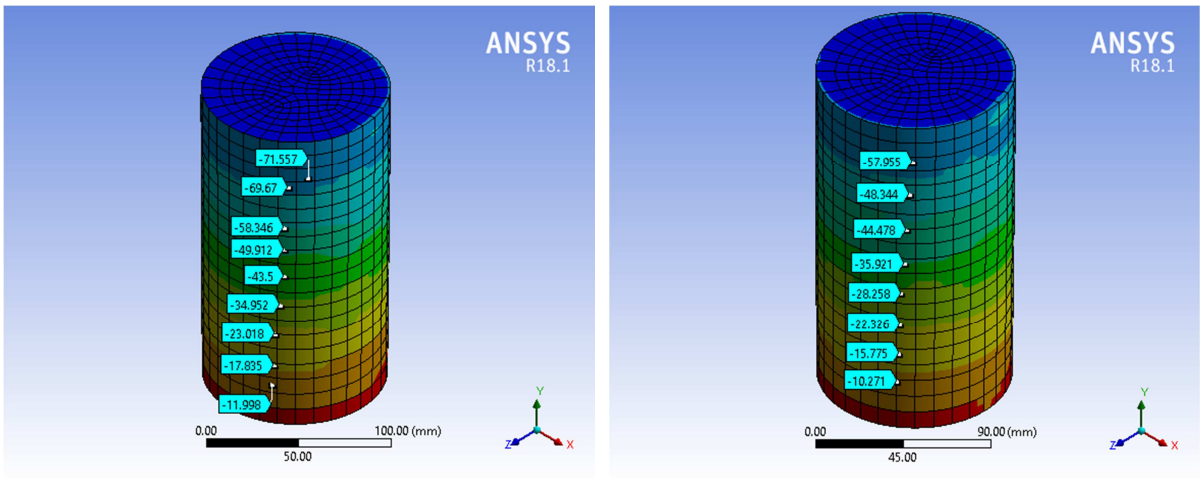

Figure 12. *Heated Compression Models. (a) CC 3 Layers; and (b) CRC 3 Layers.*

Table 4 provides a summary of the maximum and service confined compressive stresses in the models at room temperature and an elevated temperature of 120°C. Models under maximum confined compressive stress to elevated temperature experienced strength loss in the approximate range of 34% to 56% and the models under service confined compressive stress also subjected to the same elevated temperature experienced strength loss in the approximate range

of 46% to 51%. These stress losses can be attributed to concrete spalling and bursting due to loss of CFRP confinement pressure as epoxy polymer changes from a hard or brittle state to viscous or rubbery state at this elevated temperature.

Table 4. *Maximum and Service Confined Compressive Stress of Models at Room and Elevated Temperature.*

Name	f'_{cc} ***at*** $22°C$ **(MPa) – maximum**	f'_{cc} ***at*** $120°C$ **(MPa) - maximum**
CC 1 layer	79.96	47.57
CC 2 layers	119.40	64.27
CC 3 layers	139.91	92.00
CRC 1 layer	68.19	35.11
CRC 2 layers	95.17	41.54
CRC 3 layers	110.13	63.54

Name	f_{cc} ***at*** $22°C$ **(MPa) - service**	f_{cc} ***at*** $120°C$ **(MPa) - service**
CC 1 layer	48	25
CC 2 layers	72	39
CC 3 layers	84	43
CRC 1 layer	41	23
CRC 2 layers	57	28
CRC 3 layers	66	34

5. Application and Comparison of Results

FRP sheets have been widely used in recent years to provide strengthening solutions to civil engineering infrastructures that are deteriorating in strength after loading and unloading for years. Good examples are flexural strengthening of beams in bridges and compression strengthening of axially loaded columns in bridges in the United States at large. The application of FRP sheets is widely accepted because design codes are available for the design of FRP sheets for strengthening at room temperature.

The use of crumb rubber aggregates in concrete is fairly new and yet to be widely accepted but studies have shown the importance of partially replacing some aggregates with crumb rubber in concrete. There are no design codes yet for the design of FRP sheets at elevated temperature. The finite element modeling of CFRP confined concrete and crumb rubber concrete specimens at elevated temperatures using ANSYS could lead to a cost-effective, efficient and practical consideration of CFRP confined CRC in fire safety design.

An example of an axially loaded CFRP-confined CRC column with explanations to calculate the nominal load capacity of the column at room temperature and elevated temperature using the data from Table 4 is shown below.

A circular non slender CRC column of diameter 225mm and height 1500mm is reinforced with 6 numbers of steel rebar of diameter 16mm and confined with 3 layers of CFRP sheet of 0.13mm thickness per layer. f_c'= 41.6 MPa (41.6 N/mm^2), E_c= 36,434 MPa (36,434 N/mm^2), yield strength of steel rebars f_y= 414 MPa (414 N/mm^2), E_f= 2.3x10^5 MPa (2.3x10^5 N/mm^2), ε_{fu}= 0.021.

To calculate the nominal capacity of the column, we would need the 28 days confined compressive stress of the CRC (f'_{cc}), the gross area of the column (A_g) where the load is applied and the total area of steel rebars (A_{st}). The 28 days confined compressive stress for CRC confined with 3 layers of CRC as seen from Table 4 is f'_{cc}= 110.13 MPa (110.13 N/mm^2).

The gross area of column can be calculated as $A_g = \pi D_c^2/4$, where D_c is the column diameter. Hence, A_g= ($\pi \times 225^2$)/4=39761 mm^2.

The total area of the steel rebars which are 6 in numbers is given by $A_{st} = 6\pi d_b^2/4$, where d_b is the diameter of steel rebars. Therefore,

$$A_{st} = 6\pi \times 16^2/4 = 1206 \text{ mm}^2.$$

The nominal axial load capacity P_n can be calculated using equation 12-1a of ACI 440.2R-08 [19], which is as follows:

$$P_n = 0.85\left[0.85f'_{cc}\left(A_g - A_{st}\right) + f_y A_{st}\right]$$

The nominal axial load capacity of the column is calculated as:

$$P_n = 0.85[0.85 \times 110.13(39761 - 1206) + 414 \times 1206] = 3492171 \text{ N}$$

P_n at room temperature can be expressed in form of nominal axial pressure capacity of column (P_{np}) over loaded area as:

$$P_{np} = P_n/A_g = 3492171/39761 = 87.83\ MPa$$

(87.83 N/mm^2).

At an elevated temperature of 120°C, f'_{cc}= 63.54 MPa (63.54 N/mm^2) as seen from Table 4. Therefore, the nominal axial load capacity of the column can be calculated as:

$$P_n = 0.85[0.85 \times 63.54(39761 - 1206) + 414 \times 1206] = 2194361 \text{ N}$$

This P_n can also be expressed in form of nominal pressure capacity of column over loaded area as:

$P_{np} = P_n/A_g = 2194361/39761 = 55.19\ MPa$ (55.19 N/mm^2).

The above solved column is modeled in ANSYS to compare with the values of P_{np} obtained from calculations. Figure 13 shows the finite element models of pressure capacity of the column at room temperature and an elevated temperature of 120°C. The average pressure capacity estimated from the column model at room temperature is about 90.50 MPa. The percentage difference between the calculated P_{np} and the model P_{np} is $\left[\frac{90.50-87.83}{87.83}\right] * 100 \approx 3\%$.

The average pressure capacity estimated from the column model at elevated temperature of 120°C is 48.53 MPa. The percentage difference between the calculated P_{np} and the model P_{np} is

$$\left[\frac{48.53-55.19}{55.19}\right] * 100 \approx 12.1\%.$$

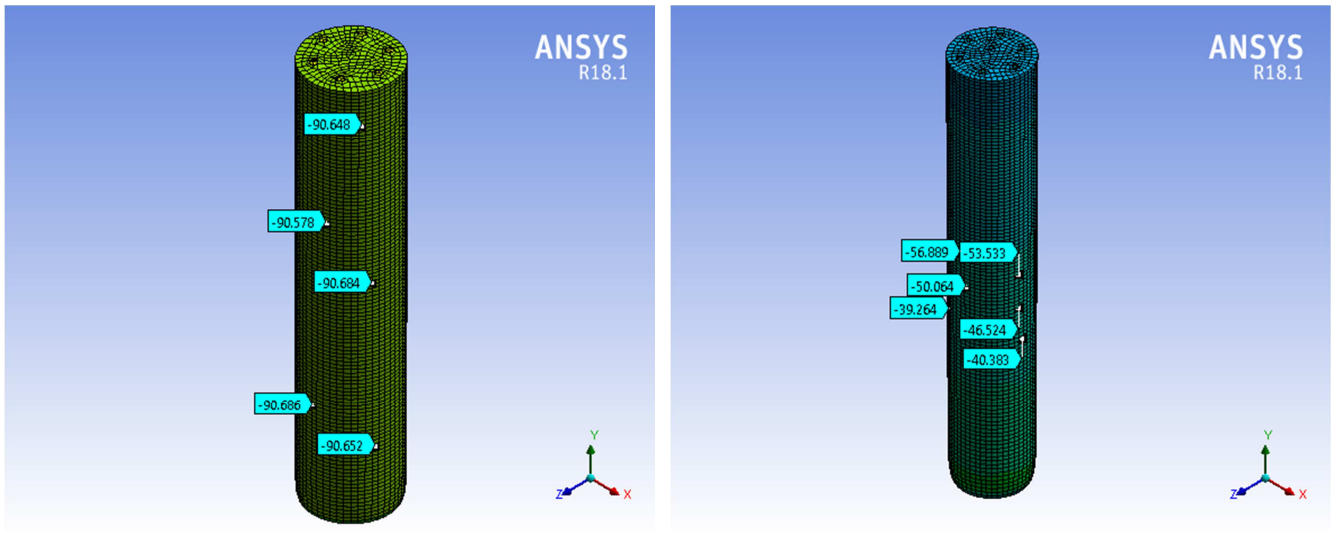

Figure 13. *Finite Element Model for Pressure Capacity of CRC Column. (a) Room Temperature; and (b) Elevated Temperature at 120°C.*

6. Conclusions and Future Studies

In this study, 14 finite element concrete models (two unconfined and 12 CFRP confined) were solved to examine the strength behavior of CRC in comparison with CC at room and elevated temperature, using material properties obtained from literature [2]. Eight finite element models were used to determine the compressive strengths at room temperature and six finite element models were used to determine service and maximum compressive stress of CFRP confined concrete specimens at a temperature within the range of practical elevated temperatures. The results of the finite element models at room temperature were compared to the results in literature and the analytical model from ACI 440.2R-08 [22]. The finite element model results were found to correlate reasonably with the literature results and the analytical model in the ACI code mentioned above. Models under maximum confined compressive stress subjected to elevated temperature experienced strength loss in the approximate range of 34% to 56% and the models under service confined compressive stress also subjected to the same elevated temperature experienced strength loss in the approximate range of 46% to 51%. These stress losses can be attributed to concrete spalling and bursting due to loss of CFRP confinement pressure at this elevated temperature.

It may be noted that this is a basic first step towards considerations in CRC fire safety designs that are efficient and cost effective. However, more experimental and theoretical work is needed. There are quite a number of ideas to be used by researchers in the future to extend the scope of this work, some of which may be to determine the effect of flammability of crumb rubber aggregate on the mechanical properties of CRC at elevated temperatures, perform experimental studies, develop analytical models, and carry out comparative analyses. All these considerations may help progress the use of CRC in strength and fire safety design.

Notations

A_g=Gross area of concrete
A_{st}=Area of steel rebar
D=Diameter of concrete specimen
D_c=Diameter of column
E_c=Young's modulus of concrete
E_f=Young's modulus of FRP
d_b=Diameter of steel rebar
f_{cc}=Service confined compressive stress of concrete under service load
f_c'=28 days maximum unconfined compressive strength of concrete
f_{cc}'=28 days maximum confined compressive strength of concrete
f_{fu}=Ultimate tensile stress of FRP sheet
f_l=Confining pressure of FRP
f_r=Concrete modulus of rupture
f_y=Yield strength of steel rebar
n=Number of FRP layers
P_n=Nominal axial load capacity of column
P_{np} =Nominal axial pressure of column due to load capacity
t_f=Thickness of FRP for one layer
T_g=Glass transition temperature of FRP

Greek Letters

ε_c=Strain in unconfined concrete
ε_{ccu}=Ultimate strain in confined concrete
ε_{fe}=Effective strain in FRP
ε_{fu}=Ultimate strain in FRP
$\emptyset$=Strength reduction factor for axial compression load
κ_a=Efficiency factor for the geometry of section
κ_ε=Efficiency factor of FRP strain
ψ_f=Additional reduction factor for confining pressure
ν=Poisson's ratio

References

[1] Rubber Manufacturers Association (2009), "Scrap Tire Markets in the United States." Ninth Biennial Report Washington DC.

[2] Osama Y, et al, (2014), "An Experimental Inv- estigation of Crumb Rubber Concrete Confined by Fiber Reinforced Polymer Tubes." Construction and Building Materials, Vol 53, pp. 522-532.

[3] Marijin, R., and Spoelstra, M., (1999), "FRP- confined Concrete Model." Journal of Composites for Construction, Vol 3 (3), pp. 143-150.

[4] Antonio. N., and Nick, B., (1995), "FRP Jacket- ed Concrete Under Uniaxial Compression." Construction and Building Materials, Vol 9 (2), pp. 115-124.

[5] Camille., I., and George, S., "Utilization of Recycled Crumb Rubber as Fine Aggregates in Concrete Mix Design." Construction and Building Materials, Vol 32, pp. 48-52.

[6] Ou, Y., et al, (2021), "Push-off and Pull-out Bond Behaviour of CRC Composite Slabs – An Experimental Investigation." Engineering Structures, 228, Article 111480.

[7] Tang, Y., et al, (2021), "Fracture Behavior of a Sustainable Material: Recycled Concrete with Waste Crumb Rubber Subjected to Elevated Temperatures." Journal of Clean Production, 318, Article 128553.

[8] Youssf, O., et al, (2022), "Mechanical Performance and Durability of Geopolymer Lightweight Rubber Concrete." Journal of Building Engineering, 45, Article 103608.

[9] Kamil, K., et al, (2005), "Properties of Crumb Rubber Concrete." Transportation Research Record. 1914: 1, pp. 8-14.

[10] Samar, R., et al, (2016), "Optimization of Rubberized Concrete with High Rubber Content: An Experimental Investigation." Construction and Building Materials, Vol 124, pp. 371- 404. ISSN 0950-0618.

[11] Piti, S., (2009), "Use of Crumb Rubber to Improve Thermal and Sound Properties of Pre-cast Concrete Panel." Construction and Building Materials, Vol 23 (2), pp. 1084-1092.

[12] Liang, Hea., et al, (2016), "Surface Modification of Crumb Rubber and its Influence on the Mechanical Properties of Rubber-cement Concre- te." Construction and Building Materials, Vol 120, pp. 403-407.

[13] Gideon, Si., et al, (2015), "Properties of Concrete Concrete with Tire Derived Aggregate Partially Replacing Coarse Aggregates." The Scientific World Journal, retrieved from http://dx.doi.org/10.1155/2015/863706.

[14] Luke, B., (2003), "Fire Behaviour of Fibre Reinforced Polymer (FRP) Reinforced Conf- ined Concrete." Queen's University Kingston Ontario, Canada Report.

[15] Najafabadi, P., et al, (2018), "Effect of Applied Stress and Bar Characteristics on the Short-term Creep Behavior of FRP Bars." Construction and Building Materials, 171: 960-968.

[16] Khaneghahi, H., et al, (2018), "Effect of Intumescent Paint Coating on Mechanical Properties of FRP Bars at elevated temperature." Polymer Testing, 71: 72-86.

[17] Najafabadi, P., et al, (2019), "The Tensile Performance of FRP Bars Embedded in Concrete Under Elevated Temperatures." Construction and Building Materials, 211: 1138-1152.

[18] Najafabadi, P., et al, (2019), "Experimental Investigation and Probabilistic Models for Residual Mechanical Properties of GFRP Pultruded Profiles Exposed to Elevated Temperature," Composites Structures, 211: 610-629.

[19] Rahai,, A., et al, (2008), "Experimental Behav- of Concrete Cylinders Confined with CFRP Composites." In: Proceeding of The 14th World Conference on Earthquake Engineering, October 12-17, Beijing, China.

[20] HuaXin, Liu., et al, (2012), "Mechanical Performance of Concrete Column Confined by BFRP Sheets Using ANSYS." In: Proceedings of Second International Conference on Electronic & Mechanical Engineering and Information Technology, September 2012, ISBN: 978-90- 78677-60-4, doi: 10.2991/emeit.2012.89.

[21] American Society of Testing Materials (ASTM) C39, (2005), "Standard Test Method for Compressive Strength of Cylindrical Concrete Specimens." Annual Book of ASTM Standards: 04.01, 21-27.

[22] American Concrete Institute (ACI) Committee 440, (2008), "Guide for the Design and Construction of Externally Bonded FRP Systems for Strengthening Concrete Structur- es." Farmington Hill, MI.

[23] Damian, K., et al, (2001), "Finite Element Modeling of Reinforced Concrete Structures with FRP Laminates." Final Report SPR 316. Oregon Department of Transportation, Research Group.

[24] Acín, G., "Stress Singularities and Concentrations-Mesh Convergence in FEA," Retrieved from: https://www.linkedin.com/pulse/stress-singularities-concentrations-mesh-fea-marcos-ac%C3%ADn-gonz%C3A1llez.

[25] Al-Salloum, Y., (2007), "Compressive Strength Models of FRP-confined Concrete." Asia-Pacific Conference on FRP in Structures, International Institute for FRP in Construction.